Photoconversion Mechanism of a Green/Red Photosensory Cyanobacteriochrome AnPixJ: Time-Resolved Optical Spectroscopy and FTIR Analysis of the AnPixJ-GAF2 Domain

ARTICLE *in* BIOCHEMISTRY · JUNE 2011

Impact Factor: 3.02 · DOI: 10.1021/bi101799w · Source: PubMed

6 AUTHORS, INCLUDING:

Yoshimasa Fukushima
Osaka City University
12 PUBLICATIONS **349** CITATIONS
SEE PROFILE

Masahiko Ikeuchi
The University of Tokyo
203 PUBLICATIONS **6,103** CITATIONS
SEE PROFILE

Shigeru Itoh
Nagoya University
222 PUBLICATIONS **4,125** CITATIONS
SEE PROFILE

BIOCHEMISTRY
including biophysical chemistry & molecular biology

ARTICLE

pubs.acs.org/biochemistry

Photoconversion Mechanism of a Green/Red Photosensory Cyanobacteriochrome AnPixJ: Time-Resolved Optical Spectroscopy and FTIR Analysis of the AnPixJ-GAF2 Domain

Yoshimasa Fukushima,[†,∥] Masayo Iwaki,[‡,⊥] Rei Narikawa,[§] Masahiko Ikeuchi,[§] Yusuke Tomita,[†] and Shigeru Itoh*[,†]

[†]Division of Material Science, Graduate School of Science, Nagoya University, Nagoya 464-8602, Japan

[‡]Glynn Laboratory of Bioenergetics, Department of Biology, University College London, Gower Street, London WC1E 6BT, U.K.

[§]Department of Life Science, Graduate School of Arts and Sciences, University of Tokyo, Tokyo 153-8902, Japan

ABSTRACT: The photoconversion mechanism of a green/red sensory cyanobacteriochrome AnPixJ was studied. The phycocyanobilin-binding second GAF domain of AnPixJ of *Anabaena* sp. PCC 7120 was expressed in *Escherichia coli* cells. The His-tagged AnPixJ-GAF2 domain exhibited photoconversion between the green- and red-absorbing forms, APg_{543} and APr_{648}, respectively. We detected four intermediate states in the photocycle between them, as follows: APr_{648} → red light → APr_{648}* → (with a rise time constant τ_r of <100 ns) $R1_{650-80}$ (with a decay time constant τ_d of <1 μs) → $R2_{610}$ (τ_d = 920 μs) → APg_{543} → green light → APg_{543}* → (τ_r < 50 ns) $G1_{570}$ (τ_d = 190 μs) → $G2_{630}$ (τ_d = 1.01 ms) → APr_{648}. These intermediates were named for their absorption peak wavelengths, which were estimated on the basis of the time-resolved difference spectra and global analysis of the time courses. The absorption spectrum of APr_{648} resembles that of the Pr form of the phytochrome, while all the other states showed peaks at 530−650 nm and had wider bandwidths with smaller peak amplitudes. The fastest decay phases of fluorescence from APr_{648}* and APg_{543}* gave lifetimes of 200 and 42 ps, respectively, suggesting fast primary reactions. The APg_{543}-minus-APr_{648} difference FTIR spectrum in an H_2O medium was significantly different from those reported for the Pfr/Pr difference spectra in phytochromes. Most of the peaks in the difference spectrum were shifted in the D_2O medium, suggesting the high accessibility to the aqueous phase. The interactions of the phycocyanobilin chromophore with the surrounding amino acid residues, which are fairly different from those in the GAF domain of phytochromes, realize the unique green/red photocycle of AnPixJ.

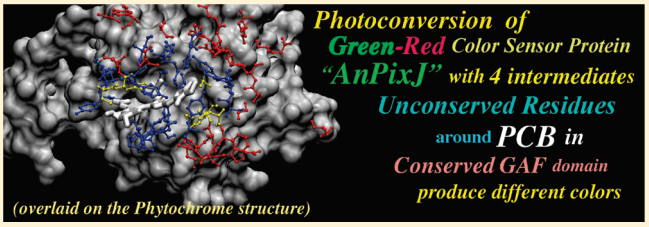

Color perception is vital for photosynthetic organisms. Phytochromes and bacteriophytochromes have been known to regulate light acclimation of plants and bacteria as red/far-red photoreceptors.[1−7] They contain GAF (cGMP-phosphodiesterase/adenylate cyclase/formate hydrogen lyase transcription activator FhlA) domains and bind bilin pigments as chromophores. Their red- and far-red-absorbing forms (Pr/Pfr forms) are well-known to be converted to each other upon red/far-red light absorption.[1,2] Multiple types of flavoproteins, such as cryptochrome, LOV, and BLUF domain proteins and photoactive yellow protein, are known to function as the blue light sensor.[8−14] Only the retinal families have been known as the green light sensor until recently, in a cyanobacterium *Anabaena* (*Nostoc*) sp. PCC 7120.[15] However, genomic analyses of cyanobacteria recently indicated another type of light sensor, cyanobacteriochromes.[16−25] Cyanobacteriochromes have GAF domains, bind bilin chromophores, and sense green/red or blue/green light.[16−25] The response to the green light, thus, seems to be a common feature of cyanobacteria.

In *Synechocystis* sp. PCC 6803 (*Synechocystis* 6803), a blue/green cyanobacteriochrome SyPixJ (PixJ1) protein[26,27] regulates the phototaxis of cells together with a BLUF photoreceptor, SyPixD.[9] Photoconversion of another blue/green sensory cyanobacteriochrome, TePixJ, of *Thermosynechococcus elongatus* BP-1 has also been reported.[18,19,25] As the green/red sensors, cyanobacteriochrome CcaS proteins of *Synechocystis* 6803 and *Nostoc punctiforme* are reported to regulate the chromatic acclimation of the photosynthetic light-harvesting system.[23,28] A cyanobacteriochrome, AnPixJ, of *Anabaena* sp. PCC 7120 also senses green/red light and is deduced to regulate the phototaxis of cells.[21]

The AnPixJ protein is composed of four GAF domains and one MCP domain. The second GAF domain (designated $AnPixJ_{GAF2}$ hereafter) binds phycocyanobilin [PCB (Figure 1C)] when expressed in *Escherichia coli* together with a pigment-synthesizing system.[21] We used the His-tagged $AnPixJ_{GAF2}$ domain expressed in *E. coli* in this study. The purified $AnPixJ_{GAF2}$ shows the green- and red-absorbing forms with peaks at 543 and 648 nm (designated APg_{543} and APr_{648}, respectively, hereafter), as shown in Figure 1A. APr_{648} gives a spectrum of the red absorption band, which resembles the absorption spectrum of the Pr form of the phytochrome that gives a peak at 667 nm with an ∼50 nm bandwidth. APr_{648} and APg_{543} interchange with each

Received: November 10, 2010
Revised: June 15, 2011
Published: June 29, 2011

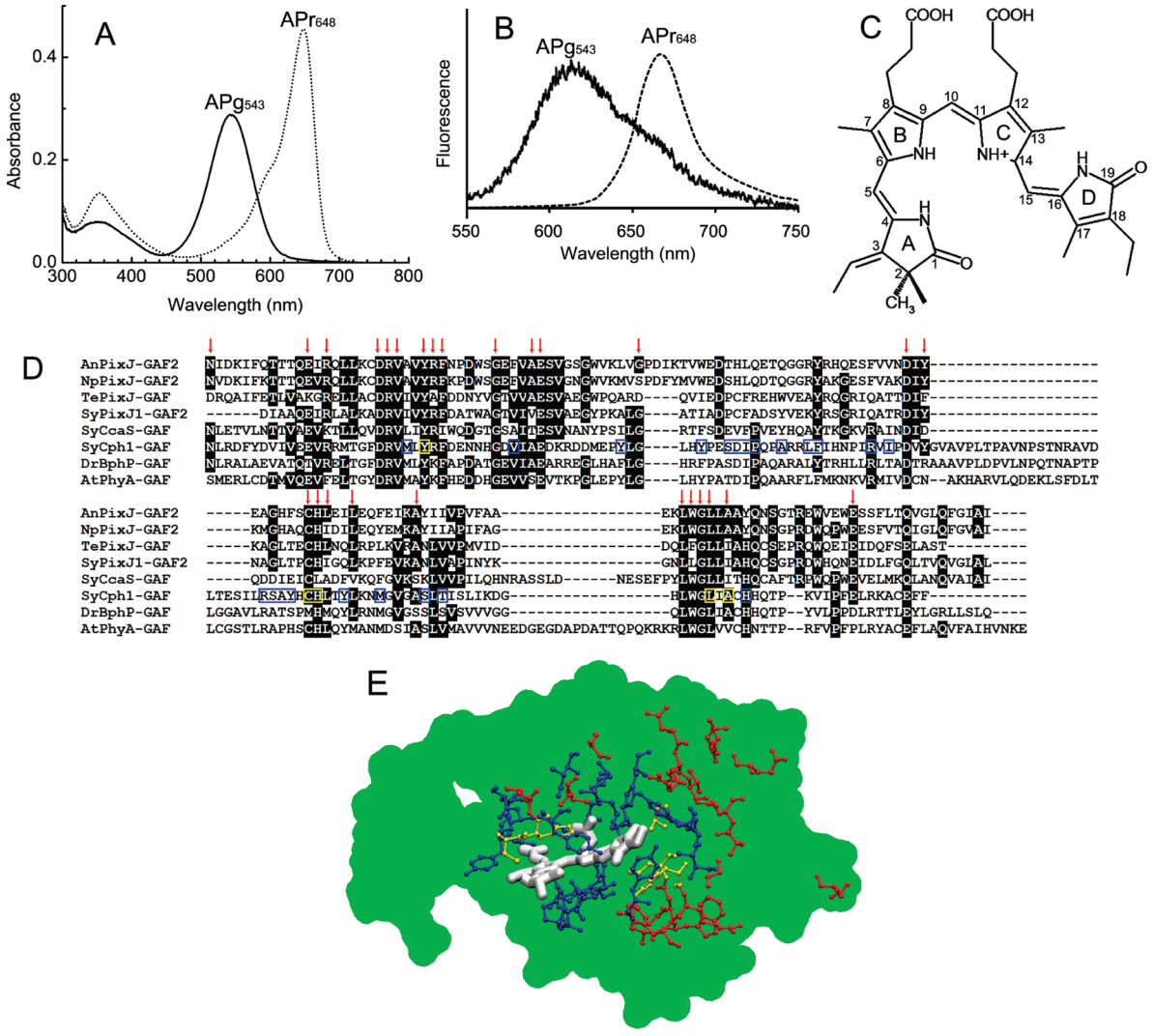

Figure 1. (A) UV−visible absorption spectra of APg_{543} (—) and APr_{648} (···) forms of $AnPixJ_{GAF2}$. (B) Fluorescence spectra of APg_{543} (—) and APr_{648} (---) forms excited at 360 and 500 nm, respectively. (C) Molecular (ZZZssa) structure of PCB. (D) Alignment of amino acid residues created with eight GAF domains of PixJs, phytochromes, and bacteriophytochromes. Residues identical among more than four GAF domains are denoted with a black background. Blue and yellow boxes represent residues forming chromophore-binding pockets in SyCph1. The residues inside blue and yellow boxes are unconserved and conserved, respectively, between $AnPixJ_{GAF2}$ and SyCph1. The residues within 5 Å of the chromophore were picked up from the structures of Pr forms of SyCph1 (Protein Data Bank entry 2VEA). Red arrows indicate the residues conserved between $AnPixJ_{GAF2}$ and SyCph1. (E) Spatial arrangements of PCB and amino acid residues on the GAF domain of SyCph1 in Pr form (Protein Data Bank entry 2VEA) that are conserved and unconserved between SyCph1-GAF and $AnPixJ_{GAF2}$. The moiety drawn as a white stick model represents the PCB chromophore, and the ball-and-stick model represents the amino acid residues shown in the homology analysis in panel D. The green part represents the whole GAF domain of SyCph1 shown in panel D. Yellow and red portions are conserved residues in contact and not in contact with PCB, respectively. Blue portions are unconserved residues in contact with PCB. Names of proteins and sequences are as follows: An, *Anabaena* (*Nostoc*) sp. PCC 7120; Np, *N. punctiforme* ATCC 29133; Te, *T. elongatus*; Sy, *Synechocystis* sp. PCC 6803; Dr, *D. radiodurans*; At, *Arabidopsis thaliana*; AnPixJ, All1069 (NP_485112); NpPixJ, NpR6012 (ZP_00110373); TePixJ, Tll0569 (NP_681359); SyPixJ1, Sll0041 (NP_442716); SyCcaS, Sll1473−1475 (ABI83649); SyCph1, Slr0473 (Q55168); DrBphP, DR_A0050 (Q9RZA4); AtPhyA, AT1G09570 (NP_172428).

other by the absorption of red and green light, respectively. The APg_{543} form is stable for several hours in the dark and converts to the APr_{648} form after a very long dark adaptation period, indicating that APr_{648} is a resting form.[21] Narikawa et al.[21] proposed a change of pigment color to reflect the isomerization of the D-ring of PCB based on the acidic urea denaturing experiment.

The amino acid sequence of $AnPixJ_{GAF2}$ shows homology to those of the GAF domains of canonical phytochromes or bacteriophytochromes, as shown in Figure 1D. The residues in the chromophore-binding pockets, which are in blue and yellow boxes in Figure 1D, are highly conserved between the sequences of cyanobacterial phytochrome Cph1 (*Synechocystis* 6803) and bacteriophytochrome DrBphP (*Deinococcus radiodurans*). Among the 27 residues that are in contact with (within 5 Å of) the PCB chromophore in the Cph1 structure, 17 residues are conserved in DrBphP. On the other hand, only five residues are common between the sequences of $AnPixJ_{GAF2}$ and Cph1 (yellow boxes, Figure 1D).

This suggests different environments and binding sites of chromophores in these proteins (see Figure 1E, too). In this

dx.doi.org/10.1021/bi101799w |*Biochemistry* 2011, 50, 6328–6339

study, we extended the analysis of the photoconversion between APr_{648} and APg_{543}, which was reported briefly in our previous report,[21] and identified the reaction times and spectral shapes of four intermediate states. We compared them to those of phytochromes to determine the mechanism of the color change and sensing of $AnPixJ_{GAF2}$. It is interesting that almost the same bilin pigments in GAF domains in the two groups of proteins undergo very different color changes.

In the Pr → Pfr photoconversion of phytochromes, three major intermediates have been proposed.[2] A sequential transition from the excited-Pr to lumi-R (with an absorption peak at 688 nm), meta-Ra (663 nm), and meta-Rc (725 nm) has been proposed in the Pr → Pfr conversion.[2] The time-resolved spectroscopy of the native oat phytochrome has revealed five kinetic components in the Pr → Pfr conversion, which are named lumi-R1, lumi-R2, meta-Ra1, meta-Ra2, and meta-Rc.[29] In the Pfr → Pr conversion, lumi-F (670 nm, 320 ns), meta-Fa (656 nm, 265 μs), and meta-Fb (660 nm, 5.5 ms) are proposed as intermediates in a sequential reaction scheme.[30]

Vibrational spectroscopy has also been used to study phytochromes in combination with isotope labeling and density functional theory calculations. The Pfr/Pr-type phytochromes showed characteristic difference FTIR spectra.[31] The phytochrome of the non-Pfr/Pr type, such as a bacteriophytochrome RpBphP3 that binds biliverdin (BV) and converts between the Pr (705 nm) and Pnr (645 nm) forms, exhibited somewhat different IR spectra.[7] Ultrafast mid-infrared spectroscopy on cyanobacterial Cph1 revealed structural changes in the picosecond time range and proposed the 15*Z* → *E* isomerization of the chromophore for the Pr → lumi-R conversion.[32] Time-resolved spectroscopy, Raman spectroscopy, and quantum chemical calculations on phytochromes also predicted the changes in the protonation state during the Pr to Pfr photoconversion.[33−35]

In this study, we identified the multiple intermediate states in the green/red photoconversion process of $AnPixJ_{GAF2}$. The intermediate states in the photoconversion of cyanobacteriochromes have not been reported yet, except for our preliminary results for $AnPixJ_{GAF2}$.[21] The results of this study identified multiple intermediates in the photocycle of $AnPixJ_{GAF2}$ and suggested the structural changes of the protein and chromophore that are fairly different from those in the photocycle of phytochromes.

MATERIALS AND METHODS

Protein Expression and Purification. His-tagged $AnPixJ_{GAF2}$ was purified as described previously.[21] *E. coli* cells that contain the expression vectors of His-tagged $AnPixJ_{GAF2}$ and chromophore expression[21,36] were harvested by centrifugation and frozen at −80 °C. The collected cells were resuspended in a 20 mM HEPES-NaOH buffer (pH 7.5) and disrupted with a French pressure cell. The disrupted cell debris was removed by centrifugation, and after imidazole had been added to the supernatant, the solution was loaded onto a Ni affinity column (HiTrap Chelating HP, GE Healthcare, Piscataway, NJ). The column was washed with a washing medium containing 20 mM HEPES-NaOH (pH 7.5), 100 mM NaCl, and 100 mM imidazole and then eluted using a step gradient of imidazole in an elution medium. The obtained protein solution was dialyzed against a reaction medium containing 20 mM HEPES-NaOH (pH 7.5), 100 mM NaCl, and 10% glycerol and stored frozen until use.

Identification of Photoconversion Intermediates by Laser Spectroscopy. The transient time course of the absorption change induced by flash excitation was measured with a home-built split beam spectrophotometer as described previously[37] with an instrument response time of 30 μs. The sample solution in an acrylic cuvette (optical path length of 10 mm) was excited by a 10 ns laser flash from SHG of a Nd:YAG laser (at 532 nm, 10 mJ; Quanta-Ray LAB-130-10TH, Spectra Physics, Santa Clara, CA) for the measurement of the APg_{543} → APr_{648} conversion or Xe flash light (10 μs duration; Sugawara Laboratories, Inc., Kawasaki, Japan) for the measurement of the APr_{648} → APg_{543} conversion at wavelengths of >620 nm through a 620 nm long-pass filter. To ensure the photoreaction from the fully converted APg_{543} or APr_{648} state, the photoproduct after each flash excitation was reversed by illumination with a 530 or 627 nm LED (LXHL-LM5C or LXHL-LD3C, respectively; Philips Lumileds Lighting, San Jose, CA). The intensity and duration of the illuminations were 16 mW/cm^2 and 1 s for the 530 nm LED and 14 mW/cm^2 and 0.25 s for the 627 nm LED, respectively. Curve fittings and global analysis of time courses were performed using Microcal Origin 6.0 (Microcal Software, Inc., Northampton, MA).

The photoconversions were also studied from shorter time ranges by measuring the time-resolved spectra with a multichannel spectrophotometer equipped with an image intensifier-gated diode array (Princeton Instruments, Trenton, NJ) or an image intensifier-gated CCD (Instaspec ICCD detector model 77193-5, ORIEL Instruments, Stratford, CT) with a time resolution of 20 or 50 ns, respectively, as reported previously.[10,37] The 10 ns excitation flash at 620 nm (at ∼1 mJ at a repetition rate of 0.03 Hz) was obtained from a solid-state dye laser (CF171 Astra, Solar TII, Minsk, Belarus), which was pumped by a 532 nm laser flash from a Nd:YAG laser (LS-2135, Solar TII). The excitation at 532 nm was conducted with the Nd:YAG laser. Time-resolved difference absorption spectra were monitored by a probing light from a 10 μs Xe flash light. The probing light that passed through the sample was diffracted in a spectrograph (MS157, ORIEL Instruments) and detected by a gated diode array or a gated ICCD detector that was controlled by a timing generator (DG535, Stanford Research Systems, Sunnyvale, CA). The diode array or the ICCD was activated for 20 or 50 ns in concert with the probing flash at varied times with respect to the laser peak time. Photoproducts formed by each excitation laser flash were, then, reverted by illuminating LED light for a few seconds following each excitation−measurement cycle as described for the time course measurement.

Measurement of Fluorescence Spectra and Lifetimes. Steady-state fluorescence spectra of APg_{543} and APr_{648} forms were measured with a fluorescence spectrometer (FL4500, Hitachi High-tech, Tokyo, Japan). Measurement of fluorescence lifetimes was conducted with a streak camera system (Hamamatsu 4334, Hamamatsu Photonics, Inc., Hamamatsu, Japan) as described previously.[38,39] APg_{543} or APr_{648} forms of an $AnPixJ_{GAF2}$ solution were excited with a SHG of a Ti:Sapphire laser at 355 nm (at 50 μW, 150 fs pulse width; Mai Tai, Spectra Physics) or a 630 nm diode laser (at 0.65 μW, 50 ps pulse width; Hamamatsu Photonics, Inc.) fired at 40 or 1 MHz, respectively, and the photons emitted from the samples were detected in a photon counting mode. The excitation beam intensities at $\sim 10^{-18}$ mol/pulse are weak enough to excite only a small fraction of the sample at a low concentration of ∼5 nmol/μL. Therefore, fluorescence is expected to be emitted from either APg_{543} or APr_{648}, and not from their doubly excited (excited intermediate) forms. We did not notice significant contributions of the intermediate fluorescence in the time-resolved spectra of

the slow decay components. The instrument response times were 21 and 50 ps for the 355 and 630 nm excitations, respectively. Acquisition of data was stopped every 5 min, and the samples were exposed to illumination with a 660 nm laser diode (1 mW/cm^2; HL6535MG, Opnext, Inc., Fremont, CA) or the 530 nm LED (0.7 mW/cm^2; LXHL-LM5C) for 1 min to fully convert the photoproducts into the initial states, in the whole measuring time of 0.5−1 h. The obtained fluorescence decay wavelength two-dimensional data were analyzed with a global analysis program as described previously.[38,39]

FTIR Measurement. The stock solution of AnPixJ$_{GAF2}$ (at ∼1 mL at ∼8 μM) was concentrated by centrifugal filtration (Vivaspin 500, 10000 molecular weight cutoff, Sartorius). The sample was diluted 10-fold with either H_2O or D_2O medium containing 20 mM HEPES and 100 mM KCl at pH or pD 7.5 and again concentrated by centrifugal filtrations. The dilution and concentration cycle was repeated two or three times to obtain the buffer-exchanged solution of AnPixJ$_{GAF2}$ at the final concentration of 0.2 mM. Samples were held at 0−10 °C during the preparation. A 5 μL aliquot of the AnPixJ$_{GAF2}$ solution was placed between two CaF_2 disks, and the disks were sealed with silicon grease and then illuminated with either a 520 or 645 nm LED to fully convert to the APr$_{648}$ or the APg$_{543}$ form, respectively. Light-induced difference FTIR spectra were recorded with a Bruker IFS66/S spectrometer equipped with a liquid nitrogen-cooled MCT-A detector as described previously,[31] which gives the spectral resolution of 4 cm^{-1} with an accuracy of ±1 cm^{-1}. After a background spectrum (an average of 400 interferograms measured for 55 s) during the 520 nm illumination had been recorded, the illumination light was switched to a 645 nm frequency, and after a 5 s delay, the sample spectrum (400 interferograms) was recorded to produce an APg$_{543}$-minus-APr$_{648}$ difference spectrum. A new background was then taken, and the light was switched back to the 520 nm LED once again. After a 5 s delay, a sample spectrum was taken during the 520 nm illumination to produce an APr$_{648}$-minus-APg$_{543}$ difference spectrum. To improve the signal-to-noise (S/N) ratio, the illumination cycle was repeated 250 times, and the obtained APg$_{543}$-minus-APr$_{648}$ spectra and the inverse of the APr$_{648}$-minus-APg$_{543}$ spectra were averaged to produce a final APg$_{543}$-minus-APr$_{648}$ spectrum. The illumination cycle was automated and synchronized with IR scanning by using a laboratory-made electric circuit. The sample was fully active during the IR measurement at 15 °C.

RESULTS

Photoconversion between APg$_{543}$ and APr$_{648}$ Forms Induced by Continuous Illumination. As shown in Figure 1A, AnPixJ$_{GAF2}$ is interconverted between the green-absorbing APg$_{543}$ and the red-absorbing APr$_{648}$ forms upon the absorption of green and red light, respectively. The conversion under continuous illumination gave isosbestic points at 582 and 452 nm, indicating the rapid interchange between these two states. The absorption band of APr$_{648}$ has a higher peak amplitude with a narrower bandwidth giving a clear shoulder. Therefore, the conversion includes a process to shift the peak and to change the spectral shape, suggesting a large change in the molecular structure of PCB inside the protein. The spectral shape of APr$_{648}$ resembles that of the Pr form of the phytochrome. The fluorescence spectra of APg$_{543}$ and APr$_{648}$ forms exhibited emission peaks at 610 and 670 nm by excitation at 360 and 500 nm, respectively (Figure 1B).

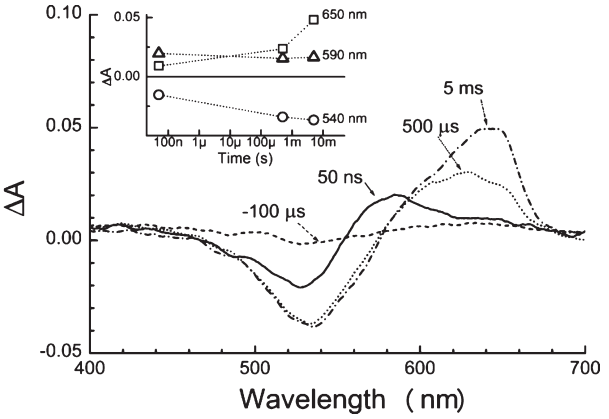

Figure 2. Time-resolved difference absorption spectra measured during the photoconversion from APg$_{543}$ to APr$_{648}$ states of AnPixJ$_{GAF2}$. Spectra were recorded with a gated diode array system at delay times of −100 μs (before the laser excitation), 50 ns, 500 μs, and 5 ms with respect to the time of excitation with a 10 ns, 532 nm laser flash. The inset shows the amplitude of the absorption change at each wavelength plotted vs the logarithm of time.

Detection of Intermediates in the Photoconversion from APg$_{543}$ to APr$_{648}$. Time-resolved difference absorption spectra were recorded with a gated diode array spectrograph to identify the reaction intermediates in the photoconversion reaction from APg$_{543}$ to APr$_{648}$ after excitation with a 10 ns laser flash at 532 nm (Figure 2). To avoid the accumulation of photoproducts during the repetitive flash excitations, the sample was illuminated with a red LED light between the excitation−measurement periods. The difference spectrum at 50 ns showed a negative peak at 530−540 nm and a positive peak at 590 nm. The difference spectrum at 500 μs showed a larger negative peak at 530−540 nm with a higher positive peak at 630 nm. The difference spectrum at 5 ms showed a similar extent of a negative peak at 540 nm and a larger positive peak at 640 nm. This difference spectrum is similar to the APr$_{648}$-minus-APg$_{543}$ difference spectrum induced by continuous illumination, indicating the formation of APr$_{648}$ from APg$_{543}$ at 5 ms. The inset shows the time-dependent changes in the amplitudes at each wavelength. These time courses and difference spectra, which differ from each other, suggested at least two intermediate states in the conversion from APg$_{543}$ to APr$_{648}$.

Time courses of the absorption changes at each wavelength were also monitored continuously after excitation with the 532 nm laser flash. In Figure 3A, the extents of absorption changes at 565, 610, and 650 nm were plotted versus the logarithm of time after laser excitation over the wide time range of 0.1−100 ms. Time courses with low noise and high time resolution were obtained by the use of 10 ns, 532 nm laser excitation, which allowed the selective excitation of APg$_{543}$. Each time course suggested multiple intermediate forms. Similar time courses measured every 10 nm from 450 to 750 nm (not shown) were, then, fitted as the sum of three exponentially decaying components and one nondecaying component. The absorption spectrum and reaction time constant of each intermediate were then assumed by a global analysis of all the time courses. The fastest kinetic component was resolved to appear with a time constant of 20 μs (i.e., within the response time of the apparatus). This component, which partially includes the contribution from

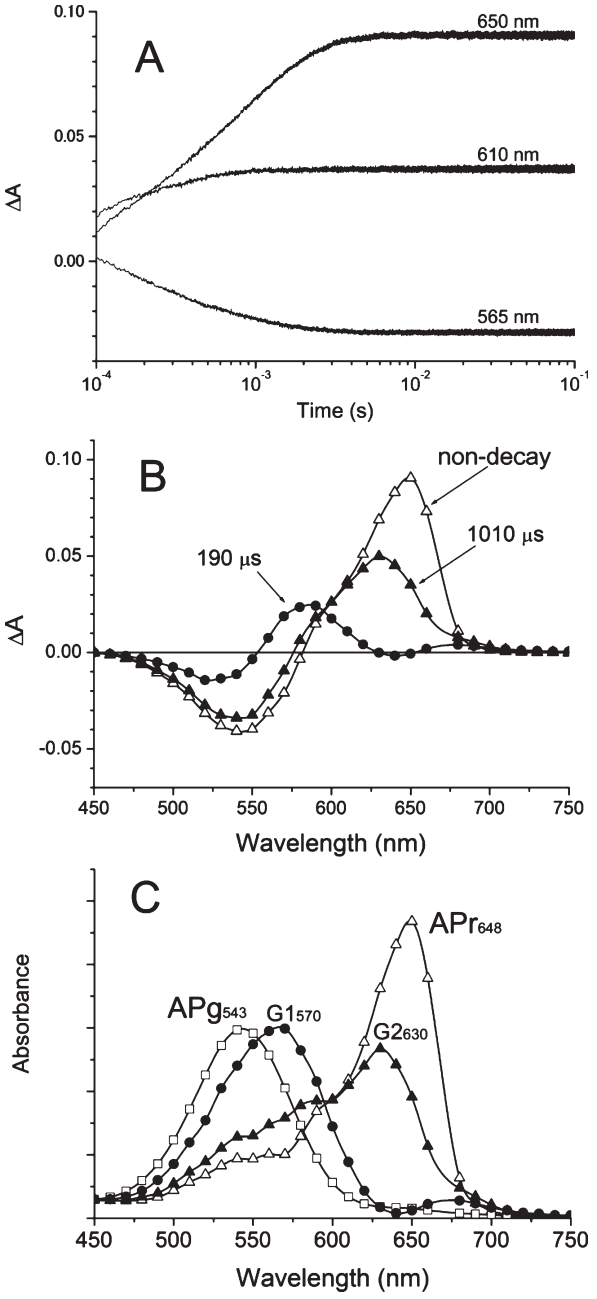

Figure 3. (A) Time courses of the absorption change at 565, 610, and 650 nm induced by the laser excitation of APg_{543}. (B) EADS of each intermediate state calculated from the set of time courses measured each 10 nm over the range of 450−750 nm. Each EADS was calculated by assuming the sequential formation of each intermediate in a single-exponential decay process. Filled circles and triangles represent the EADS with 190 μs (G1) and 1010 μs (G2) decay time constants, respectively. Empty triangles represent the photoproduced nondecaying component. (C) The absorption spectrum of each intermediate state was estimated by adding each EADS sequentially to the absorption spectrum (□) of APg_{543} with appropriate normalizations as described in the text. Filled circles, filled triangles, and empty triangles represent the estimated absorption spectra of the 190 μs (G1), 1010 μs (G2), and nondecay (APr_{648}) components, respectively.

the fluorescence from the excited state of APg_{543}, was not further analyzed. The two slower components, which had decay time constants of 190 and 1010 μs, were further analyzed.

We analyzed the amplitudes of the 190 μs (τ_1) and 1010 μs (τ_2) decay phases at all wavelengths to obtain the absorption spectra of reaction intermediates. Figure 3B shows the evolution-associated difference spectra (EADS) obtained by assuming a simple scheme and rate equations, in which sequential reactions take place as follows

$$APg_{543}^* \rightarrow \rightarrow G1\ (\tau_1 = 190\ \mu s) \rightarrow$$
$$G2\ (\tau_2 = 1010\ \mu s) \rightarrow APr_{648}$$

where τ_1 and τ_2 represent the lifetimes of two intermediate states. The EADS with a τ_1 of 190 μs had a negative peak at 520 nm and a positive one at 590 nm (the intermediate state is designated G1). The spectrum is almost the same as the time-resolved spectrum at 50 ns in Figure 2 and indicates the formation of the G1 state from APg_{543} within 50 ns of laser excitation and its conversion to the second intermediate (G2) with a time constant (τ_1) of 190 μs (see Discussion).

The second EADS with a τ_2 of 1010 μs showed a negative peak at 540 nm and a positive peak at 630 nm with a shoulder at ~590 nm. The difference spectrum indicates the red shift of the peak wavelength of the absorption band from 543 nm in APg_{543} to 590 nm in G1 and then to 630 nm in G2. The difference spectrum of the nondecaying component showed a negative peak at 540 nm and a positive peak at 650 nm. It was almost the same as that of the APr_{648}-minus-APg_{543} difference spectrum obtained at the steady state. These results indicate that the transition from G2 to APr_{648} takes place with a τ_2 of 1010 μs.

The absorption spectra of G1 and G2 were estimated by adding each EADS spectrum to the (steady-state) absorption spectrum of APg_{543} by using an adequate normalization factor that was calculated from the comparison of "the nondecaying component of EADS" and "the APr_{648}-minus-APg_{543} difference spectrum" (Figure 3C). The absorption spectra of APg_{543}, G1, G2, and APr_{648} showed peaks at 543, 570, 630, and 648 nm, respectively. It is clear that the photoconversion proceeds with the hopping of peak wavelengths from 543 nm to the red until 648 nm is reached in ~0.1 s, together with the changes in the conformation of the protein. The spectra of APg_{543} and G1 show similar bandwidths and peak amplitudes with 27 nm-shifted peak wavelengths. The estimated G2 spectrum gave a peak at 630 nm with a similar or slightly smaller peak amplitude and a wider bandwidth. The spectral feature of G2 might also contain small contributions from G1 and APr_{648} because the wide bandwidth of G2 extended to the spectral ranges of these states. This may happen if the actual decays do not obey single exponentials. On the other hand, it is clear that APr_{648} has a higher peak amplitude and a narrower bandwidth compared to the other states. This suggests a significant change in the chromophore structure in the conversion from G2 to APr_{648}.

Detection of Intermediates in the Photoconversion from APr_{648} to APg_{543}. Time-resolved difference absorption spectra were also recorded in the photoconversion from APr_{648} (Figure 4). We measured the difference spectrum at each indicated time after the 20 ns, 620 nm laser-flash excitation by using the gated ICCD to eliminate the effect of flash-induced strong fluorescence from APr_{648}. After each excitation−measurement period, photoproduced APg_{543} was converted back to APr_{648} via illumination of the green 530 nm LED light for 1 s to suppress the accumulation of photoproducts.

One hundred nanoseconds after the laser excitation of APr_{648}, we obtained a difference spectrum with a positive peak at 680 nm (indicated by the arrow marked a in Figure 4) and a large negative peak at 650 nm as reported previously.[21] The negative peak

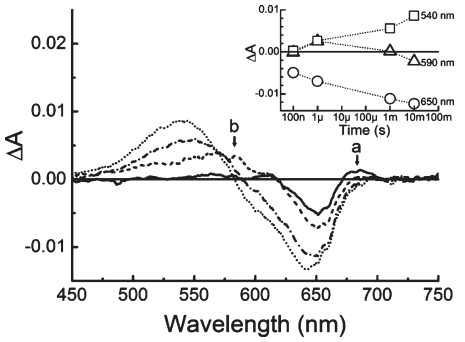

Figure 4. Time-resolved difference absorption spectra measured at 100 ns (—), 1 μs (– – –), 1 ms (-·-·-), and 10 ms (···) after laser excitation at 620 nm on the APr_{648} form of $AnPixJ_{GAF2}$. Arrows marked a and b denote the positions of apparent peaks at 680 and 570 nm, respectively. The inset shows the amplitude of the absorption change at each wavelength plotted vs the logarithm of time.

represents the bleaching of the ground state of the APr_{648} band. The positive peak suggests the formation of a new intermediate, R1, which represents the formation of either a red-shifted band with a peak at 682 nm, as indicated by arrow a, or an intermediate at almost the same peak wavelength with a lower amplitude and wider bandwidth extended to the red side as discussed further below. The difference spectrum recorded at 1 μs had no 680 nm positive peak and showed a broad positive peak at ~570 nm (indicated by arrow b), suggesting the formation of the second intermediate (R2) from R1 (Figure 4). At a delay time of 1 ms, the amplitude of the negative band around 650 nm increased more, and the positive peak was further blue-shifted to 550 nm. Ten milliseconds after excitation, the positive band showed a peak at 540 nm, indicating the conversion to the final APg_{543} form. The inset time courses in Figure 4 indicate that an early intermediate R1 with a peak or shoulder at 680 nm is formed from APr_{648} within 100 ns of the laser excitation and the second intermediate R2 is then formed within 1 μs.

We also measured the time course of the absorption change of APr_{648} induced by the excitation with a 10 μs xenon flash (>620 nm) in the 100 μs to 100 ms time range at each wavelength (Figure 5A). The large noise levels mainly came from the use of a fast response amplifier and the attenuated intensity of a probing light with the use of a monochromator to eliminate the broad and long scattering light and fluorescence induced by the xenon flash, the intensity of which was also low because of the limitation of the experimental setup for this measurement. The averaging and smoothing of abundant data points by an appropriate program, however, allowed detailed analysis of the time courses, especially over the longer time range. The whole process of photoconversion was completed within 5 ms of flash excitation. At 510 nm, the excitation induced only a small increase at the beginning and then gradually increased. At 580 nm, the instantaneous increase was larger, and the extent then gradually decreased.

We measured similar time courses each 10 nm over a range of 450−750 nm and calculated the EADS after analyzing each time course as a sum of decaying components that appear in a series. The analysis produced the difference absorption spectrum of an intermediate component (R2), which decays with a time constant of 920 μs, together with the nondecaying one, which corresponds to the formation of APg_{543}, as shown in Figure 5B. The analysis of the time courses also indicated the formation of an R1 intermediate before R2, although the reaction time from

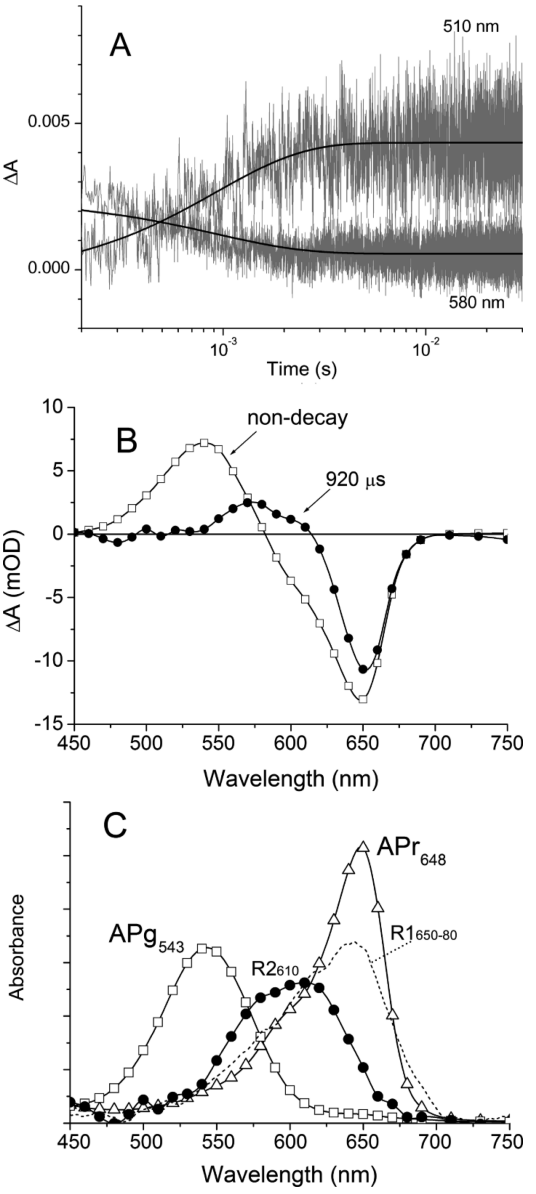

Figure 5. (A) Time courses of absorption change at 580 and 610 nm after the excitation of APr_{648} with the red xenon flash. (B) EADS calculated from the time courses every 10 nm, like those in panel A, at 450−750 nm by assuming the sequential single-pathway scheme. Filled circles and empty squares represent the 920 μs decay component (R2) and the nondecaying component, respectively. (C) Absorption spectra of intermediates estimated by adding each difference spectrum or EADS to the steady-state absorption spectrum of APr_{648} (△). The dotted line represents the tentative absorption spectrum of R1. Filled circles and empty squares represent the estimated absorption spectra of the 920 μs decay (R2) and nondecaying (APg_{543}) components, respectively.

R1 to R2 within 10 μs could not be determined precisely because of the disturbance from the fluorescence excited by the long tail of the xenon flash. We used the time-resolved spectra in Figure 4 as well for the construction of the whole reaction process. On the basis of the results in Figures 4 and 5A, we assumed that the whole reaction process proceeds sequentially as follows.

$$APr_{648}^{*} \rightarrow \rightarrow R1\ (\tau_1 \simeq 1\ \mu s) \rightarrow$$
$$R2\ (\tau_2 = 920\ \mu s) \rightarrow APg_{543}$$

dx.doi.org/10.1021/bi101799w |*Biochemistry* 2011, 50, 6328–6339

The absorption spectra of intermediates R1 and R2 (dashed line and filled circles, respectively, in Figure 5C) were calculated by adding the difference spectrum/EADS to the steady-state APr_{648} spectrum after adequate normalization. The spectrum of R1, which was estimated on the basis of the time-resolved spectrum in Figure 4, represents the results in Figure 5 well. The simulation result gave a spectrum with a peak amplitude lower than that of APr_{648} with the shoulder extended to 680 nm rather than a spectrum with a red-shifted peak at 680 nm, although the result is still tentative. The spectrum of R2 is significantly blue-shifted to 610 nm. The peak amplitude of the R2 band after normalization is significantly lower than that of APr_{648} and is close to that of APg_{543}. These results suggest that R1 has a lower peak amplitude at ~648 nm with a bandwidth wider than that of APr_{648}. The peak wavelength then shifted to 610 nm in R2 and to 543 nm in APg_{543}, showing similar peak amplitudes. The simulated absorption spectra of R1 and R2 intermediates are different from those of G1 and G2, suggesting different changes in chromophore configuration in the forward and backward photoconversions between APr_{648} and APg_{543}.

Fluorescence Lifetimes of APr_{648} and APg_{543}. The fluorescence spectra of APg_{543} and APr_{648} forms in Figure 1B showed emission peaks at 610 and 670 nm, respectively. To estimate the rates of the initial photoconversions from the excited states of APr_{648} (APr_{648}*) and APg_{543} (APg_{543}*), we measured the fluorescence lifetimes by using a streak camera system. We measured the wavelength−lifetime two-dimensional image of fluorescence after the excitation of APr_{648} at 630 nm with a 50 ps diode laser pulse or APg_{543} at 355 nm with a 0.2 ps pulse from a Ti:sapphire laser. A global analysis of the data points in different wavelength−time regions could resolve the decay time courses of multiple emission components even under the mixing conditions, as reported previously.[38,39]

The fluorescence from APr_{648} gave decay times of 200 ps (70% in amplitude) and 1000 ps (30%). APg_{543}, on the other hand, showed faster decay times of 42 ps (60%) and 610 ps (40%), as listed in Table 1. The time resolutions of the measurement of the APr_{648} and APg_{543} fluorescence were 50 and 21 ps, respectively. We assume the decay time constants of the major fast components in both states to be related to the photoconversion reactions and those of the slower components to be derived either from a heterogeneity or back reaction from the primary intermediates. The fluorescence of the Pr form of the phytochrome is reported to give two or more kinetic components,[40,41] in which the fastest 30−60 ps component depended on the viscosity of the medium.[40] Biphasic decay was interpreted either by the heterogeneity of the sample or the fluorescence (delayed fluorescence) from the light-formed intermediate because of the reversibility of the reaction.[40]

Recent studies by the ultrafast transient absorption measurement of the bacteriophytochrome RpBphP3 estimated the fast quenching process from Pr* to occur with a 350 ps time constant because of the proton transfer−back-shuttle reaction between the chromophore (BV) and the amino acid, based on the observation of the slower rate in the D_2O medium.[42] The fast fluorescence lifetimes of APr_{648}* and APg_{543}* may represent similar quenching mechanisms. The question of whether APr_{648}* and APg_{543}* are converted to R1 and G1 directly with time constants of 200 and 42 ps, respectively, or via some other early intermediates that cannot be detected at 50−100 ns by the present measurement of the absorption change remains to be answered.

Table 1. Fluorescence Lifetimes of APr_{648}* and APg_{543}*[a]

fluorescence-emitting form (fluorescence peak wavelength)	lifetime (initial amplitude, relative)		
APr_{648}* (670 nm)	200 ps (0.7)	1000 ps (0.3)	
APg_{543}* (610 nm)	42 ps (0.6)	610 ps (0.4)	
Pr* (680 nm)[b]	39.6 ps (0.90)	167 ps (0.09)	1145.0 ps (0.01)

[a] The lifetimes and relative initial amplitudes of decay components were calculated by the global analyses of wavelength−time two-dimensional images of the fluorescence as described in Materials and Methods. [b] Pr of 124 kDa oat phytochrome measured in potassium phosphate buffer (pH 7.8).[40]

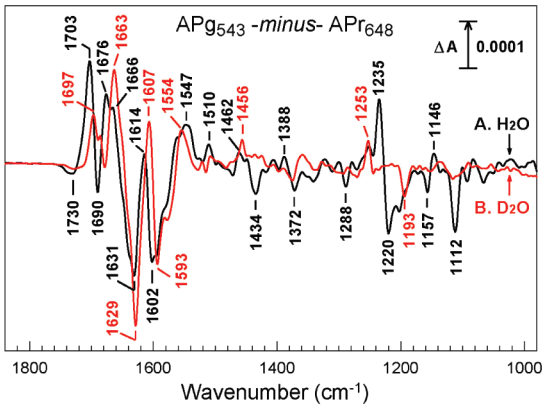

Figure 6. APg_{543}-minus-APr_{648} difference FTIR spectra of $AnPixJ_{GAF2}$. Light-induced difference spectra of $AnPixJ_{GAF2}$ were recorded in H_2O (A, black) and D_2O (B, red) media [20 mM HEPES and 100 mM KCl (pH or pD 7.5)] at 15 °C. The APr_{648} and APg_{543} forms were generated by continuous illumination with 520 and 645 nm LEDs, respectively.

APg_{543}-Minus-APr_{648} Difference FTIR Spectra. We measured the FTIR difference spectra of $AnPixJ_{GAF2}$ induced by illumination with an either green (520 nm) or red (645 nm) LED. The APg_{543}-minus-APr_{648} difference spectra, which were calculated from the 250 illumination cycles in H_2O and D_2O media, are shown in Figure 6. The difference spectrum in H_2O medium showed major bands at 1703(+), 1690(−), 1676(+), 1631(−), 1602(−), 1235(+), 1220(−), and 1112(−) cm^{-1} (Figure 6A). The IR features were drastically altered by the H−D exchange (Figure 6B). All the IR bands listed above were modified in their amplitudes and/or frequencies as well as the minor bands at 1547(+), 1510(+), 1434(−), 1388(+), 1372(−), 1288(−), 1157(+), and 1146(+) cm^{-1}. The obtained APg_{543}-minus-APr_{648} difference spectra in H_2O and D_2O are significantly different from those reported for Pfr/Pr-type phytochromes,[31] a Pnr/Pr-type bacteriophytochrome, RpBphP3,[7] and a Pg/Pb-type cyanobacteriochrome, TePixJ.[25]

DISCUSSION

Features of Cyanobacteriochrome $AnPixJ_{GAF2}$ and Phytochrome. A cyanobacteriochrome $AnPixJ_{GAF2}$ undergoes unique green/red photoconversion.[21] The feature is apparently different from that of red/far-red conversion in phytochromes.[1,2] Other green sensory cyanobacteriochromes are a blue/green type,

Scheme 1. Photoconversion between APg_{543} and APr_{648}

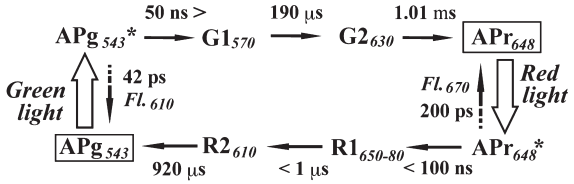

cyanobacteriochrome TePixJ, of *T. elongatus*[18,19,25] and a green/red type, CcaS of *Synechocystis* and *Nostoc*, that regulate the chromatic adaptation.[23,28] Therefore, the ability of cyanobacteriochromes to sense green light seems to be important for the light adaptation of cyanobacteria, which have multiple photosynthetic pigments, such as phycobilins, carotenoids, and chlorophyll *a*, to harvest light from the whole visible region.

The absorption spectrum of APg_{543} in Figure 1A resembles that of the green-absorbing forms of TePixJ,[18,25] although the photoconversion intermediates of the latter have not yet been identified. On the other hand, the absorption spectrum of APr_{648} is quite similar to that of the Pr forms of phytochromes and bacteriophytochromes,[2] showing a high peak amplitude and narrow bandwidth. It is noteworthy that the photoconversions start from APr_{648} and Pr to the blue and red sides, respectively. We, therefore, compare the photoconversion processes of APr_{648} and Pr in detail in the following sections.

The results of this study confirm those in our previous report[21] and indicate that each photoconversion process of $AnPixJ_{GAF2}$ proceeds with two metastable intermediate states that can be detected 50 ns to 1 s after the laser or flash excitation. The photocycle with multiple intermediates shown in this study clearly resembles that of phytochrome.[2,29,30] However, the features of the intermediates differ from each other. Narikawa et al. showed that $AnPixJ_{GAF2}$ binds PCB based on an acidic urea denaturation experiment.[21] PCB is also contained in the cyanobacterial phytochrome Cph1 of *Synechocystis*, which shows the photochromism between Pr and Pfr forms as seen in plant phytochromes.[43] The same PCB chromophore, thus, shows different color changes in different GAF domains. This is probably due to the interactions of identical PCBs with different protein environments inside these GAF domains.[21] On the other hand, the shape and peak wavelength of the absorption spectrum of APr_{648} are very similar to those of the Pr form of the phytochrome. This suggests that the PCB configurations of APr_{648} are similar to the structure of the Pr form revealed by X-ray crystallography.[44] We summarize the green/red photocycle of APr_{648} below and discuss its reaction mechanism further on the basis of the kinetic results and FTIR measurements.

Photocycle of $AnPixJ_{GAF2}$ with Four Intermediate States. Each conversion from APg_{543} or APr_{648} occurred with two semistable intermediate states, as summarized in Scheme 1. We named the intermediate states in Scheme 1 according to the order of appearance and their estimated peak wavelengths. We identified intermediates $G1_{570}$ and $G2_{630}$ in the conversion from APg_{543} and $R1_{650-80}$ (which was designated as APi_{680} previously in ref 21) and $R2_{610}$ in the conversion from APr_{648}.

The peak positions of all the intermediates, except for $R1_{650-80}$ in Scheme 1, were different from those of the intermediates reported in the photoconversion of phytochrome, which gave peaks at 650−720 nm.[2,29,30] APr_{648} has an absorption spectrum with the highest peak amplitude and the narrowest bandwidth in all four intermediates and APg_{543}. The spectral shape of APr_{648} resembles that of the Pr form of the phytochrome.

Fluorescence emitted from APr_{648}* showed a peak at 670 nm with a Stokes shift of 22 nm and a lifetime of 200 ps. The lifetime is longer than the 30−60 ps lifetimes of the Pr forms of oat and pea phytochromes, which depended on the buffer and viscosity conditions.[40] From APr_{648}*, $R1_{650-80}$ was formed within 100 ns, and $R1_{650-80}$ was then converted to the second intermediate, $R2_{610}$, with a time constant of ∼1 μs. $R1_{650-80}$ may be formed either directly from APr_{648}* with a time constant comparable to 200 ps or indirectly via some other early unidentified intermediate. Simulations in this study suggested the spectrum of $R1_{650-80}$ (Figure 5C) has a peak at ∼650 nm and a broad bandwidth extending to 680 nm. This spectrum can realize the difference spectrum, although we previously assumed $R1_{650-80}$ to have a peak at 680 nm.[21] We still cannot totally ignore the possibility that the difference spectrum at 100 ns is a mixture of $R1_{650-80}$ with another earlier intermediate that has a peak at ∼680 nm. Therefore, we tentatively express the intermediate as $R1_{650-80}$ in Scheme 1. Further measurements with a shorter delay time or at low temperatures may give a clearer spectral shape of R1.

The absorption change associated with the APr_{648}* → $R1_{650-80}$ process can be compared to that with the Pr* → lumi-R process of phytochromes or Cph1. The lumi-R intermediate form of the phytochrome has an absorption peak at 690−700 nm, at a wavelength longer than that of Pr.[2,29,45] In Cph1, its lumi-R spectrum was assumed to have almost the same peak position as that of Pr with a lower absorption amplitude.[46] If lumi-R and $R1_{650-80}$ share similar optical properties, then we expect similar configuration changes of the PCB pyrrole rings between lumi-R of Cph1 and $R1_{650-80}$ of $AnPixJ_{GAF2}$ because the spectrum of APr_{648} is very similar to that of Pr of the cyanobacterial phytochrome Cph1. Then, the reaction mechanism in the first photoconversion process in $AnPixJ_{GAF2}$ might be the $Z \leftrightarrow E$ isomerization at the C15═C16 bond during the formation of $R1_{650-80}$ in analogy to the interpretation of lumi-R formation.[1,2,32]

$R2_{610}$ is assumed to have a peak at 610 nm. This indicates a blue shift from $R1_{650-80}$ to $R2_{610}$ in the second step of the conversion. This blue shift gives a marked contrast to the red shifts between the intermediates in the Pr-to-Pfr photoconversion process of phytochromes and bacteriophytochromes.[2,29] The blue shift of the absorption band of $R2_{610}$ suggests the localization (and/or appearance of nodal character) of the π-orbital on PCB to the smaller region due to the movement of the pyrrole ring(s) to the nonplanar orientation(s) within 1 μs.

The third step was the larger blue shift of the peak from 610 to 543 nm in the conversion from $R2_{610}$ to APg_{543}. This suggests the further localization of the π-orbital on PCB, probably by the further movements forming the nonplanar conformation of pyrrole rings. In $AnPixJ_{GAF2}$, further rotation of the A-ring may twist the plane of the pyrrole ring(s) to be out of the major molecular π-orbital plane in this step.

APg_{543}* gave a fluorescence peak at 610 nm, which is distant from the absorption peak at 543 nm with a large Stokes shift of 70 nm, suggesting its complex excited state. APg_{543}* fluorescence gave a lifetime of 42 ps, as shown in Table 1. This fast lifetime is comparable to the 30−60 ps lifetime of the Pr* of the phytochrome.[40,41] APg_{543}* produced $G1_{570}$ within 50 ns. If we assume the quantum yield of the photoconversion of $AnPixJ_{GAF2}$ to be similar to those reported for the Pr−Pfr conversion of the

phytochrome at ~0.1,[32,43,47] then the initial photoconversion reaction, which competes with the fluorescence-emitting process, will have a reaction time constant of a few hundred picoseconds. We can, thus, assume that $G1_{570}$ is formed either directly with a time constant of a few hundred picoseconds or via another earlier intermediate that is formed with this short time constant and then converted to $G1_{570}$ within 50 ns. $G1_{570}$ turned into $G2_{630}$ with a time constant of 190 μs, and then $G2_{630}$ turned into APr_{648} with a longer time constant of 1010 μs. The latter process was the slowest one in the whole photoconversion cycle of $AnPixJ_{GAF2}$ and was accompanied by an increase in the absorption peak amplitude.

APg_{543}, $G1_{570}$, $G2_{630}$, and $R2_{610}$ states (i.e., all the states except $R1_{650-80}$ and APr_{648}) are very different from the intermediates detected in the photoconversion of canonical phytochromes, which have no such blue-shifted intermediates.[2,29,30] We can, however, find the short wavelength peaks in *Agrobacterium* Agp1 and Agp2 reconstituted with synthesized pigments.[48,49] The absorption spectra of Agp1 and Agp2 with "15*Zs*" and "15*Es*" locked BV, in which the C15═C16 bond was fixed in the *Z*/*E* configuration and the C14−C15 bond in the *syn* conformation, showed peaks at ~430 nm. No intermediate of $AnPixJ_{GAF2}$ showed such a blue peak. On the other hand, Agp2 reconstituted with a "5*Za*" synthetically locked chromophore, which is a BV derivative with the C4═C5 bond fixed in the *Z* configuration and the C5−C6 bond in an *anti* conformation, showed the absorption peak at 640 nm. This peak wavelength is close to that of $G2_{630}$ of $AnPixJ_{GAF2}$. The configuration of PCB in $G2_{630}$ might resemble this conformation, although further studies with AnPixJ should be conducted to confirm it.

Structural Changes of the Pigment and Protein in the Photoconversion of $AnPixJ_{GAF2}$. In the reaction of Cph1 and phytochromes, several reports proposed the $Z \leftrightarrow E$ isomerization at the C15═C16 bond (of the D-ring) in the conversion from Pr to Pfr.[1,2,32] X-ray structural analysis of α-phycoerythrocyanin also suggested the $Z \leftrightarrow E$ isomerization at the C15═C16 bond of phycoviolobilin to be responsible for the shift of the peak from 500 nm (15*E*) to 580 nm (15*Z*).[50] A recent NMR study of the cyanobacterial phytochrome of *Synechococcus* OSB′ proposed a different mechanism, namely, that the isomerization of the A-ring of PCB is responsible for the conversion from the Pr form to the Pfr form.[51] Although no comparable experimental results exist for AnPixJ at present, we can assume the isomerization (rotation) of the pyrrole ring(s) on either side edge of PCB to be responsible for the conversion to the shorter wavelength. APr_{648} showed the sequential blue shifts in the conversion to APg_{543}, while the Pr of the phytochrome or bacteriophytochrome with a similar absorption spectrum shows the red shift in the photoconversion to Pfr. Therefore, the changes in configuration of the PCB chromophores in $AnPixJ_{GAF2}$ and phytochromes seem to differ in the chromophore−protein interactions.

The APg_{543}-minus-APr_{648} difference FTIR spectrum showed features (Figure 6) that were significantly different from those reported for the photoconversion of phytochromes, TePixJ, Agp1, and RpBphP3.[7,25,31] Although the information obtained in this study is limited, we tentatively assigned the IR peaks/troughs as described below by comparing the spectrum with that of the Pr/Pfr-type cyanobacterial phytochrome, Cph1, which also contains PCB.[31] It is known that the Pfr/Pr-type phytochromes present a marker band of the Pfr state at 1650−1656 cm^{-1}. In the Pfr-minus-Pr spectrum of Cph1, the most prominent band was detected at 1653 cm^{-1}. This band was less sensitive to the H−D exchange as well as to the specific isotope labeling of the PCB itself and thus can be assigned primarily to amide I of the α-helical structure of the protein.[31] In the amide I region of $AnPixJ_{GAF2}$ spectra, no such marker band was evident. We, therefore, assumed that the IR feature at 1666(+)/1631(−) cm^{-1}, which was less sensitive to H−D exchange, reflects the changes in the amide I and/or chromophore C═C vibrational modes. A remarkable negative band in the amide I region was also resolved in the FTIR spectrum of the domain-truncated Agp1.[52] The Pfr-minus-Pr difference spectrum of the Agp1-M15 protein, which is composed of the chromophore module (PLD, GAF, and PHY domains) and lacks the His-kinase module, shows a negative band at 1635 cm^{-1}. The apparent similarity of the negative band in the amide I region (1631 cm^{-1} in $AnPixJ_{GAF2}$ and 1635 cm^{-1} in Agp1-M15) might represent a similarity in protein architecture between APr_{648} of $AnPixJ_{GAF2}$ and Pr of Agp1-M15.

In the carbonyl C═O stretch region of the Pfr-minus-Pr difference spectrum of Cph1, the bands at 1736(−)/1724(+) and 1704(−) cm^{-1} were assigned to the carbonyl groups of PCB pyrrole ring-A and ring-D, respectively, on the basis of the effects of H−D exchange and specific isotope labeling on PCB. In $AnPixJ_{GAF2}$, IR bands at 1730(−), 1703(+), 1690(−), and 1676(−) cm^{-1}, which were sensitive to H−D exchange, could have arisen from the vibrational modes of the protonated and/or hydrogen-bonded chemical groups. On the other hand, in an analogy to the cases in Cph1[31] and/or phyA,[52] the 1730(−), 1703(+), and 1602(−) cm^{-1} bands could be assigned to the structural changes in PCB ring-A and ring-D and the B−C bridge, respectively. The 1690(−)/1676(+) cm^{-1} feature might be assigned to the propionate of PCB. In a lower-frequency region, the prominent IR features at 1235(+)/1220(−) and 1112(−) cm^{-1}, which were apparently lost in the D_2O medium, seem to be assigned to the C−N vibrational modes of PCB according to ref 31 in which the IR bands in this region were tentatively assigned to the C−N mode of PCB in Cph1. In the case of Agp1-M15, a band shift at 1244(−)/1233(+) cm^{-1} has been resolved in the Pfr-minus-Pr spectrum.[53] These trough/peak positions are close to those of $AnPixJ_{GAF2}$ [1235(+)/1220(−) cm^{-1}], but the direction of the shift is opposite. These results indicate that the chromophore−protein interaction in $AnPixJ_{GAF2}$ is largely different from that in phytochromes, in agreement with the prediction from the analysis of the visible spectral changes. It was also reported that B-deprotonated tetrapyrrole shows a downshift in the IR band at 1224 cm^{-1} (A-ring N−H in-plane bending) by DFT calculations.[53] Thus, the band pair at 1235(+)/1220(−) cm^{-1} may be derived from the change in protonation state between APr_{648} and APg_{543}, although it is difficult to assign at present. It is noteworthy that deprotonation and protonation take place, as proposed for the Pr → Pfr conversion of phytochromes,[35] during the photoconversion of $AnPixJ_{GAF2}$.

We tested the structural difference between phytochromes and $AnPixJ_{GAF2}$ on the basis of their amino acid sequences, shown in Figure 1D on the structure of the former. The residues shown in Figure 1D are shown in Figure 1E in the ball-and-stick model to elucidate their location on the known structure of the Pr form of SyCph1. The residues, which are homologous to those of $AnPixJ_{GAF2}$, are colored red and yellow, and those that are not conserved in $AnPixJ_{GAF2}$ and are in contact with PCB are colored blue. PCB drawn in the stick model is colored white. The image shows that the residues in contact with PCB (within 5 Å) are

rather unconserved (colored blue) except for a few conserved residues that are colored yellow. The majority of conserved residues, which are colored red, are far from PCB. The distributions of conserved and unconserved residues, therefore, seem to support the conclusions from the FTIR studies and intermediate analyses in this study that assessed the interaction between the PCB chromophore and protein to be significantly different from that in phytochromes. The unique unconserved residues in contact with PCB seem to represent the unique photoconversion mechanism of $AnPixJ_{GAF2}$. Nature, thus, has created different color sensory systems in cyanobacteriochromes and phytochromes by almost fully modifying the amino acid residues just in contact with the pigment within the homologous outer shell of the GAF domains.

Photoconversion Mechanism of $AnPixJ_{GAF2}$. $AnPixJ_{GAF2}$ undergoes the photoconversion cycle between its red and green forms with four intermediate states as shown in Scheme 1, i.e., two intermediate states in each direction. The feature with the stepwise peak shifts in each direction resembles that of phytochromes and bacteriophytochromes and the other photoreceptors in which isomerization of the pigment takes place.[12] The phytochrome photoconversion has been assumed to accompany the $Z \leftrightarrow E$ isomerization at a C15=C16 bond. The movement of similar pyrrole ring(s) (presumably the D-ring) may also occur in APr_{648}. The peak wavelengths of $R2_{610}$, $G1_{570}$, and $G2_{630}$ in the $AnPixJ_{GAF2}$ cycle, however, are apparently different from those of intermediates in the photocycles of phytochromes. To realize the shorter wavelength peaks of intermediates, different molecular mechanisms, such as unique movements and/or rotations of pyrrole A- or D-rings, may occur in $AnPixJ_{GAF2}$. The reconstitution of pigments with locked configurations, like that in Agp1 and Agp2,[48,49] will be useful in understanding its photoconversion mechanism.

The FTIR difference spectrum of $AnPixJ_{GAF2}$, which is significantly different from those of phytochromes, suggests the interaction between the PCB chromophore and $AnPixJ_{GAF2}$ proteins to be somewhat different from that of phytochromes. The multiple vibrational modes were sensitive to the photoconversion and to H−D exchange, suggesting the high accessibility of protein and chromophore side bands to water in $AnPixJ_{GAF2}$, although the PCB configurations in the APr_{648} and Pr forms appear to be similar according to their similar absorption spectra. This may suggest a slightly exposed location of PCB in $AnPixJ_{GAF2}$. The homology of the amino acid residues visualized in Figure 1E clearly indicates that the outer shell structure of the GAF domain is well-conserved, while the chromophore-surrounding residues, including the ligand residues, are significantly modified. The unique feature of the photocycle of $AnPixJ_{GAF2}$, thus, seems to be realized by the variations of the residues that surround and ligate the PCB pigment. The high degree of sensitivity to H−D exchange also suggests the shift of the PCB location closer to the outer aqueous phase from that in Figure 1E.

$AnPixJ_{GAF2}$ was recently crystallized,[54] and its structure in the APr_{648} form will be revealed soon. A preliminary analysis indicated that PCB shows a configuration similar to that of Cph1 in the Pr form in a shifted binding position (R. Narikawa, N. Muraki, T. Shiba, G. Kurisu, and M. Ikeuchi, unpublished result), which agrees with the conclusion of this study. Analyses based on the structure will further advance our understanding of the photoconversion mechanism of green/red or blue/green sensing by cyanobacteriochromes and may also extend our understanding of the photoconversion mechanism of phytochromes. We will be able to design the proteins with a variety of colors and reaction modes with this knowledge.

AUTHOR INFORMATION

Corresponding Author

*E-mail: itoh@bio.phys.nagoya-u.ac.jp. Phone: +81(52) 789 4739. Fax: +81(52) 789 4739.

Present Addresses

[||]The Center for Gene Research, Nagoya University, Nagoya 464-8602, Japan.

[⊥]Toyota Central R&D Laboratories Inc., Yokomichi, Nagakute, Aichi 480-1192, Japan.

Funding Sources

This work has been supported by grant-in-aid for challenging exploratory research to S.I. (23655196) from MEXT.

ACKNOWLEDGMENT

We thank Drs. Peter R. Rich and Santiago Garcia (University College London) for their kind assistance with the FTIR measurement and Dr. Masahiro Ishiura in the Center for Gene Research of Nagoya University and Dr. Kosuke Maki in the Department of Physics of Nagoya University for their kind support of the research.

ABBREVIATIONS

APg_{543} and APr_{648}, green- and red-absorbing forms of the second GAF domain of AnPixJ, respectively; BV, biliverdin; EADS, evolution-associated difference spectrum; FTIR, Fourier transform infrared spectroscopy; GAF, cGMP-phosphodiesterase/*Anabaena* adenylyl-cyclase/*E. coli* formate hydrogen lyase transcription activator; PCB, phycocyanobilin; Pr and Pfr, red- and far-red-absorbing forms of the phytochrome, respectively.

REFERENCES

(1) Rockwell, N. C., Su, Y.-S., and Lagarias, J. C. (2006) Phytochrome structure and signaling mechanisms. *Annu. Rev. Plant Biol. 57*, 837–858.

(2) Tu, S.-L., and Lagarias, J. C. (2005) The phytochromes. In *Handbook of Photosensory Receptors* (Briggs, W. R., and Spudich, J. L., Eds.) pp 121−149, Wiley-VCH, Weinheim, Germany.

(3) Yeh, K.-C., Wu, S.-H., Murphy, J. T., and Lagarias, J. C. (1997) A cyanobacterial phytochrome two-component light sensory system. *Science 277*, 1505–1508.

(4) Bhoo, S.-H., Davis, S. J., Walker, J., Karniol, B., and Vierstra, R. D. (2001) Bacteriophytochromes are photochromic histidine kinases using a biliverdin chromophore. *Nature 414*, 776–779.

(5) Wilde, A., Fiedler, B., and Börner, T. (2002) The cyanobacterial phytochrome Cph2 inhibits phototaxis towards blue light. *Mol. Microbiol. 44*, 981–988.

(6) Wilde, A., Churin, Y., Schubert, H., and Börner, T. (1997) Disruption of a *Synechocystis* sp. PCC 6803 gene with partial similarity to phytochrome genes alters growth under changing light qualities. *FEBS Lett. 406*, 89–92.

(7) Giraud, E., Zappa, S., Vuillet, L., Adriano, J.-M., Hannibal, L., Fardoux, J., Berthomieu, C., Bouyer, P., Pignol, D., and Verméglio, A. (2005) A new type of bacteriophytochrome acts in tandem with a classical bacteriophytochrome to control the antennae synthesis in *Rhodopseudomonas palustris*. *J. Biol. Chem. 280*, 32389–32397.

(8) Gomelsky, M., and Klug, G. (2002) BLUF: A novel FAD-binding domain involved in sensory transduction in microorganisms. *Trends Biochem. Sci. 27*, 497–500.

(9) Okajima, K., Yoshihara, S., Fukushima, Y., Geng, X., Katayama, M., Higashi, S., Watanabe, M., Sato, S., Tabata, S., Shibata, Y., Itoh, S., and Ikeuchi, M. (2005) Biochemical and functional characterization of BLUF-type flavin-binding proteins of two species of cyanobacteria. *J. Biochem. 137*, 741–750.

(10) Fukushima, Y., Okajima, K., Shibata, Y., Ikeuchi, M., and Itoh, S. (2005) Primary intermediate in the photocycle of a blue-light sensory BLUF FAD-protein, Tll0078, of *Thermosynechococcus elongatus* BP-1. *Biochemistry 44*, 5149–5158.

(11) Salomon, M., Christie, J. M., Knieb, E., Lempert, U., and Briggs, W. R. (2000) Photochemical and mutational analysis of the FMN-binding domains of the plant blue light receptor, phototropin. *Biochemistry 39*, 9401–9410.

(12) van der Horst, M. A., and Hellingwerf, K. J. (2004) Photoreceptor proteins, "star actors of modern times:" A review of the functional dynamics in the structure of representative members of six different photoreceptor families. *Acc. Chem. Res. 37*, 13–20.

(13) Narikawa, R., Zikihara, K., Okajima, K., Ochiai, Y., Katayama, M., Shichida, Y., Tokutomi, S., and Ikeuchi, M. (2006) Three putative photosensory light, oxygen or voltage (LOV) domains with distinct biochemical properties from the filamentous cyanobacterium *Anabaena* sp. PCC 7120. *Photochem. Photobiol. 82*, 1627–1633.

(14) Hoff, W. D., van Stokkum, I. H., van Ramesdonk, H. J., van Brederode, M. E., Brouwer, A. M., Fitch, J. C., Meyer, T. E., van Grondelle, R., and Hellingwerf, K. J. (1994) Measurement and global analysis of the absorbance changes in the photocycle of the photoactive yellow protein from *Ectothiorhodospira halophila*. *Biophys. J. 67*, 1691–1705.

(15) Jung, K.-H., Trivedi, V. D., and Spudich, J. L. (2003) Demonstration of a sensory rhodopsin in eubacteria. *Mol. Microbiol. 47*, 1513–1522.

(16) Yoshihara, S., Katayama, M., Geng, X., and Ikeuchi, M. (2004) Cyanobacterial phytochrome-like PixJ1 holoprotein shows novel reversible photoconversion between blue- and green-absorbing forms. *Plant Cell Physiol. 45*, 1729–1737.

(17) Yoshihara, S., Shimada, T., Matsuoka, D., Zikihara, K., Kohchi, T., and Tokutomi, S. (2006) Reconstitution of blue-green reversible photoconversion of a cyanobacterial photoreceptor, PixJ1, in phycocyanobilin-producing *Escherichia coli*. *Biochemistry 45*, 3775–3784.

(18) Ishizuka, T., Shimada, T., Okajima, K., Yoshihara, S., Ochiai, Y., Katayama, M., and Ikeuchi, M. (2006) Characterization of cyanobacteriochrome TePixJ from a thermophilic cyanobacterium *Thermosynechococcus elongatus* BP-1. *Plant Cell Physiol. 47*, 1251–1261.

(19) Ishizuka, T., Narikawa, R., Kohchi, T., Katayama, M., and Ikeuchi, M. (2007) Cyanobacteriochrome TePixJ of *Thermosynechococcus elongatus* harbors phycoviolobilin as a chromophore. *Plant Cell Physiol. 48*, 1385–1390.

(20) Ikeuchi, M., and Ishizuka, T. (2008) Cyanobacteriochromes: A new superfamily of tetrapyrrole-binding photoreceptors in cyanobacteria. *Photochem. Photobiol. Sci. 7*, 1159–1167.

(21) Narikawa, R., Fukushima, Y., Ishizuka, T., Itoh, S., and Ikeuchi, M. (2008) A novel photoactive GAF domain of cyanobacteriochrome AnPixJ that shows reversible green/red photoconversion. *J. Mol. Biol. 380*, 844–855.

(22) Rockwell, N. C., Njuguna, S. L., Roberts, L., Castillo, E., Parson, V. L., Dwojak, S., Lagarias, J. C., and Spiller, S. C. (2008) A second conserved GAF domain cysteine is required for the blue/green photoreversibility of cyanobacteriochrome Tlr0924 from *Thermosynechococcus elongatus*. *Biochemistry 47*, 7304–7316.

(23) Hirose, Y., Shimada, T., Narikawa, R., Katayama, M., and Ikeuchi, M. (2008) Cyanobacteriochrome CcaS is the green light receptor that induces the expression of phycobilisome linker protein. *Proc. Natl. Acad. Sci. U.S.A. 105*, 9528–9533.

(24) Narikawa, R., Kohchi, T., and Ikeuchi, M. (2008) Characterization of the photoactive GAF domain of the CikA homolog (SyCikA, Slr1969) of the cyanobacterium *Synechocystis* sp. PCC 6803. *Photochem. Photobiol. Sci. 7*, 1253–1259.

(25) Ulijasz, A. T., Cornilescu, G., von Stetten, D., Cornilescu, C., Velazquez Escobar, F., Zhang, J., Stankey, R. J., Rivera, M., Hildebrandt, P., and Vierstra, R. D. (2009) Cyanochromes are blue/green light photoreversible photoreceptors defined by a stable double cysteine linkage to a phycoviolobilin-type chromophore. *J. Biol. Chem. 284*, 29757–29772.

(26) Yoshihara, S., Suzuki, F., Fujita, H., Geng, X., and Ikeuchi, M. (2000) Novel putative photoreceptor and regulatory genes required for the positive phototactic movement of the unicellular motile cyanobacterium *Synechocystis* sp. PCC 6803. *Plant Cell Physiol. 41*, 1299–1304.

(27) Yoshihara, S., and Ikeuchi, M. (2004) Phototactic motility in the unicellular cyanobacterium *Synechocystis* sp. PCC 6803. *Photochem. Photobiol. Sci. 3*, 512–518.

(28) Hirose, Y., Narikawa, R., Katayama, M., and Ikeuchi, M. (2010) Cyanobacteriochrome CcaS regulates phycoerythrin accumulation in *Nostoc punctiforme*, a group II chromatic adapter. *Proc. Natl. Acad. Sci. U.S.A. 107*, 8854–8859.

(29) Zhang, C.-F., Farrens, D. L., Björling, S. C., Song, P.-S., and Kliger, D. S. (1992) Time-resolved absorption studies of native etiolated oat phytochrome. *J. Am. Chem. Soc. 114*, 4569–4580.

(30) Chen, E., Lapko, V. N., Lewis, J. W., Song, P.-S., and Kliger, D. S. (1996) Mechanism of native oat phytochrome photoreversion: A time-resolved absorption investigation. *Biochemistry 35*, 843–850.

(31) van Thor, J. J., Fisher, N., and Rich, P. R. (2005) Assignments of the Pfr-Pr FTIR difference spectrum of cyanobacterial phytochrome Cph1 using ^{15}N and ^{13}C isotopically labeled phycocyanobilin chromophore. *J. Phys. Chem. B 109*, 20597–20604.

(32) van Thor, J. J., Ronayne, K. L., and Towrie, M. (2007) Formation of the early photoproduct lumi-R of cyanobacterial phytochrome Cph1 observed by ultrafast mid-infrared spectroscopy. *J. Am. Chem. Soc. 129*, 126–132.

(33) Mizutani, Y., Tokutomi, S., and Kitagawa, T. (1994) Resonance Raman spectra of the intermediates in phototransformation of large phytochrome: Deprotonation of the chromophore in the bleached intermediate. *Biochemistry 33*, 153–158.

(34) Mroginski, M. A., Murgida, D. H., and Hildebrandt, P. (2007) The chromophore structural changes during the photocycle of phytochrome: A combined resonance Raman and quantum chemical approach. *Acc. Chem. Res. 40*, 258–266.

(35) Borucki, B., von Stetten, D., Seibeck, S., Lamparter, T., Michael, N., Mroginski, M. A., Otto, H., Murgida, D. H., Heyn, M. P., and Hildebrandt, P. (2005) Light-induced proton release of phytochrome is coupled to the transient deprotonation of the tetrapyrrole chromophore. *J. Biol. Chem. 280*, 34358–34364.

(36) Mukougawa, K., Kanamoto, H., Kobayashi, T., Yokota, A., and Kohchi, T. (2006) Metabolic engineering to produce phytochromes with phytochromobilin, phycocyanobilin, or phycoerythrobilin chromophore in *Escherichia coli*. *FEBS Lett. 580*, 1333–1338.

(37) Iwaki, M., Itoh, S., Kamei, S., Matsubara, H., and Oh-oka, H. (1999) Time-resolved spectroscopy of chlorophyll-*a* like electron acceptor in the reaction center complex of the green sulfur bacterium *Chlorobium tepidum*. *Plant Cell Physiol. 40*, 1021–1028.

(38) Komura, M., and Itoh, S. (2009) Fluorescence measurement by a streak camera in a single-photon-counting mode. *Photosynth. Res. 101*, 119–133.

(39) Komura, M., Yamagishi, A., Shibata, Y., Iwasaki, I., and Itoh, S. (2010) Mechanism of strong quenching of photosystem II chlorophyll fluorescence under drought stress in a lichen, *Physciella melanchla*, studied by subpicosecond fluorescence spectroscopy. *Biochim. Biophys. Acta 1797*, 331–338.

(40) Song, P.-S., Singh, B. R., Tamai, N., Yamazaki, T., Yamazaki, I., Tokutomi, S., and Furuya, M. (1989) Primary photoprocesses of phytochrome. Picosecond fluorescence kinetics of oat and pea phytochromes. *Biochemistry 28*, 3265–3271.

(41) Holzwarth, A. R., Wendler, J., Ruzsicska, B. P., Braslavsky, S. E., and Schaffner, K. (1984) Picosecond time-resolved and stationary

fluorescence of oat phytochrome highly enriched in the native 124 kDa protein. *Biochim. Biophys. Acta 791*, 265–273.

(42) Toh, K. C., Stojković, E. A., van Stokkum, I. H. M., Moffat, K., and Kennis, J. T. M. (2010) Proton-transfer and hydrogen-bond interactions determine fluorescence quantum yield and photochemical efficiency of bacteriophytochrome. *Proc. Natl. Acad. Sci. U.S.A. 107*, 9170–9175.

(43) Lamparter, T., Mittmann, F., Gärtner, W., Börner, T., Hartmann, E., and Hughes, J. (1997) Characterization of recombinant phytochrome from the cyanobacterium *Synechocystis*. *Proc. Natl. Acad. Sci. U.S.A. 94*, 11792–11797.

(44) Essen, L.-O., Mailliet, J., and Hughes, J. (2008) The structure of a complete phytochrome sensory module in the Pr ground state. *Proc. Natl. Acad. Sci. U.S.A. 105*, 14709–14714.

(45) Kendrick, R. E., and Spruit, C. J. P. (1977) Phototransformations of phytochrome. *Photochem. Photobiol. 26*, 201–214.

(46) Heyne, K., Herbst, J., Stehlik, D., Esteban, B., Lamparter, T., Hughes, J., and Diller, R. (2002) Ultrafast dynamics of phytochrome from the cyanobacterium *Synechocystis*, reconstituted with phycocyanobilin and phycoerythrobilin. *Biophys. J. 82*, 1004–1016.

(47) Lagarias, J. C., Kelly, J. M., Cyr, K. L., and Smith, W. O. (1987) Comparative photochemical analysis of highly purified 124 kDa oat and rye phytochromes *in vitro*. *Photochem. Photobiol. 46*, 5–13.

(48) Inomata, K., Hammam, M. A. S., Kinoshita, H., Murata, Y., Khawn, H., Noack, S., Michael, N., and Lamparter, T. (2005) Sterically locked synthetic bilin derivatives and phytochrome Agp1 from *Agrobacterium tumefaciens* form photoinsensitive Pr- and Pfr-like adducts. *J. Biol. Chem. 280*, 24491–24497.

(49) Inomata, K., Noack, S., Hammam, M. A. S., Khawn, H., Kinoshita, H., Murata, Y., Michael, N., Scheerer, P., Krauss, N., and Lamparter, T. (2006) Assembly of synthetic locked chromophores with *Agrobacterium* Phytochromes Agp1 and Agp2. *J. Biol. Chem. 281*, 28162–28173.

(50) Schmidt, M., Patel, A., Zhao, Y., and Reuter, W. (2007) Structural basis for the photochemistry of α-phycoerythrocyanin. *Biochemistry 46*, 416–423.

(51) Ulijasz, A. T., Cornilescu, G., Cornilescu, C. C., Zhang, J., Rivera, M., Markley, J. L., and Vierstra, R. D. (2010) Structural basis for the photoconversion of a phytochrome to the activated Pfr form. *Nature 463*, 250–254.

(52) Schwinté, P., Foerstendorf, H., Hussain, Z., Gärtner, W., Mroginski, M.-A., Hildebrandt, P., and Siebert, F. (2008) FTIR study of the photoinduced processes of plant phytochrome PhyA using isotope-labeled bilins and density functional theory calculations. *Biophys. J. 95*, 1256–1267.

(53) Piwowarski, P., Ritter, E., Hofmann, K.-P., Hildebrandt, P., von Stetten, D., Scheerer, P., Michael, N., Lamparter, T., and Bartl, F. (2010) Light-induced activation of bacterial phytochrome Agp1 monitored by static and time-resolved FTIR spectroscopy. *Chem. Phys. Chem. 11*, 1207–1214.

(54) Narikawa, R., Muraki, N., Shiba, T., Ikeuchi, M., and Kurisu, G. (2009) Crystallization and preliminary X-ray studies of the chromophore-binding domain of cyanobacteriochrome AnPixJ from *Anabaena* sp. PCC 7120. *Acta Crystallogr. F65*, 159–162.